Electronic Supplementary Information (ESI)

Multifunctional tris(triazolo)triazine-based emitter with dual-TADF, RTP, AIEE and AIDF properties

Marli Ferreira,[§*a] Nícolas Oliveira Decarli,[§b] Aleksandra Nyga,[a] Karol Erfurt,[c] Jaijanarthanan Lingagouder,[d] Leonardo Evaristo de Sousa,[e] Laure de Thieulloy,[e] Piotr de Silva,[*e] and Przemyslaw Data[*d]

* Corresponding author

§ These authors contributed equally to the experimental work.

[a.] Centre for Organic and Nanohybrid Electronics, Silesian University of Technology, Konarskiego 22B, 44-100, Gliwice, Poland. E-mail: marli.ferreira@polsl.pl

[b.] Department of Physical Chemistry and Technology of Polymers, Faculty of Chemistry, Silesian University of Technology, M. Strzody 9, 44-100 Gliwice, Poland.

[c.] Department of Chemical Organic Technology and Petrochemistry, Faculty of Chemistry, Silesian University of Technology, B. Krzywoustego 4, 44-100 Gliwice, Poland.

[d.] Department of Molecular Physics, Faculty of Chemistry, Łódź University of Technology, Stefana Żeromskiego 114, 90-543 Łódź, Poland. E-mail: przemyslaw.data@p.lodz.pl

[e.] Department of Energy Conversion and Storage, Technical University of Denmark, Kongens Lyngby, Denmark. E-mail: pdes@dtu.dk

Contents

1. General considerations 2
2. Supplementary photophysical data 3
2.1 Time-resolved spectroscopic analysis 3
2.2 Electronic structure calculations 4
2.3 Ultraviolet-visible absorption and photoluminescence spectra 4
2.4 Simulation of fluorescence spectrum of TTT-PTZ 4
3. OLED devices additional data 5
4. Experimental section 6
4.1 Synthetic procedures and spectroscopy data 6
5. Copies of NMR Charts of final compounds 9
6. Computational details 12
7. References 13

1. General considerations

All solvents and materials were used as received from commercial sources without further purification.

Column chromatography was performed using 60 Å silica-gel 230-400 mesh from Supelco and 60 Å neutral aluminium oxide, Brockmann I, 40-300 µm from Acros Organics. Thin-layer chromatography (TLC) was performed using TLC Silica gel 60 F254 plates (Merck KGaA) and the materials were visualized with UV lamp (245 nm, 365 nm).

NMR spectra were recorded on a Varian 300 MHz spectrometer (^{1}H NMR: 300 MHz, ^{13}C{^{1}H} NMR: 75 MHz) and the NMR data was processed in MestReNova.

High-resolution mass spectrometry (HRMS) analyses were performed on a Waters Xevo G2 Q-TOF mass spectrometer (Waters Corporation) equipped with an ESI source operating in positive-ion modes. Full-scan MS data were collected from 100 to 5000 Da in positive ion mode with a scan time of 0.1 s. To ensure accurate mass measurements, data were collected in centroid mode and mass was corrected during acquisition using leucine enkephalin solution as an external reference (Lock-Spray TM), which generated reference ion at m/z 556.2771 Da ($[M+H]^{+}$) in positive ESI mode. The accurate mass and composition for the molecular ion adducts were calculated using the MassLynx software (Waters) incorporated with the instrument.

The electrochemical investigations were carried out using Eco Chemie Company's AUTOLAB potentiostat "PGSTAT20". The results were collected using GPES (General Purpose Electrochemical System) software. The electrochemical cell comprised of the platinum wire electrode as a working electrode for electrochemical measurements, Ag wire electrode as a reference electrode and platinum coil as an auxiliary electrode. The electrochemical measurements were performed using 1.0 mM of the emitters in 0.1 M tetrabutylammonium tetrafluoroborate (Bu_4NBF_4) in anhydrous dichloromethane or anhydrous tetrahydrofuran. Cyclic voltamperometric measurements were conducted at room temperature in the glovebox at a scan rate of 50 mV/s and were calibrated against ferrocene/ferrocenium redox couple.

Absolute photoluminescence quantum yields were determined using a HAMAMATSU C11347-01 spectrometer with an integrating sphere. Solid state samples were prepared with 1% w/w ratio TTT-emitters in Zeonex® matrix or 10% CBP host on sapphire disc substrates. Phosphorescence, prompt fluorescence (PF), and delayed fluorescence (DF) spectra and fluorescence decay curves were recorded using nanosecond gated luminescence and lifetime measurements (from 400 ps to 1 s) using either third harmonics of a high energy pulsed DPSS laser emitting at 355 nm (Q-Spark-A50). Emission was focused onto a spectrograph and detected on a sensitive gated iCCD camera (Stanford Computer Optics) having sub-nanosecond resolution. PF/DF time-resolved measurements were performed by exponentially increasing gate and integration times. Temperature photophysical measurements were conducted in Janis CCS-450 closed cycle helium cytostatic system.

2. Supplementary photophysical data

2.1 Time-resolved spectroscopic analysis

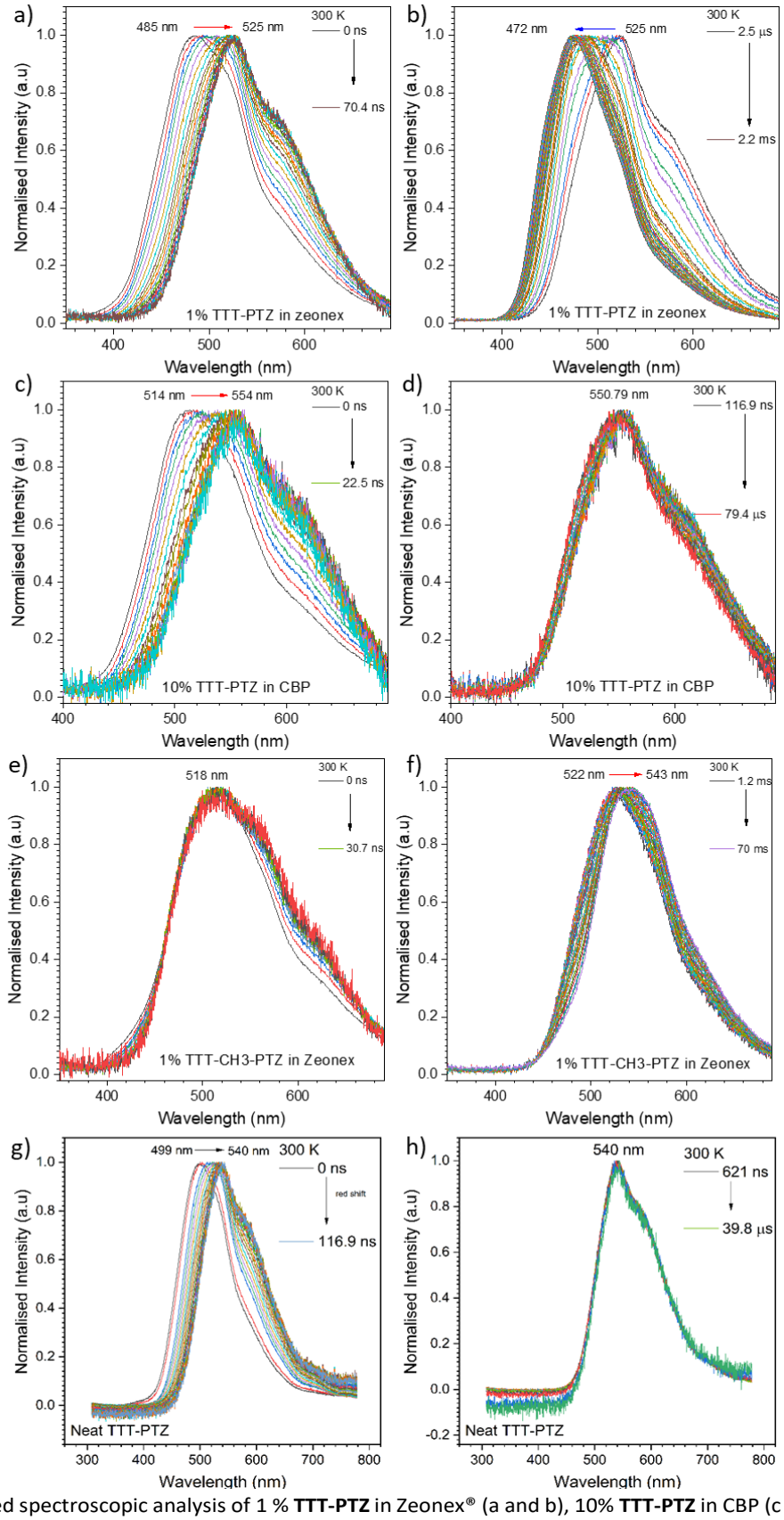

Figure S1. Time-resolved spectroscopic analysis of 1 % **TTT-PTZ** in Zeonex® (a and b), 10% **TTT-PTZ** in CBP (c and d), 1 % **TTT-CH3-PTZ** in Zeonex® (e and f), and neat **TTT-PTZ** (g and h).

2.2 Electronic structure calculations

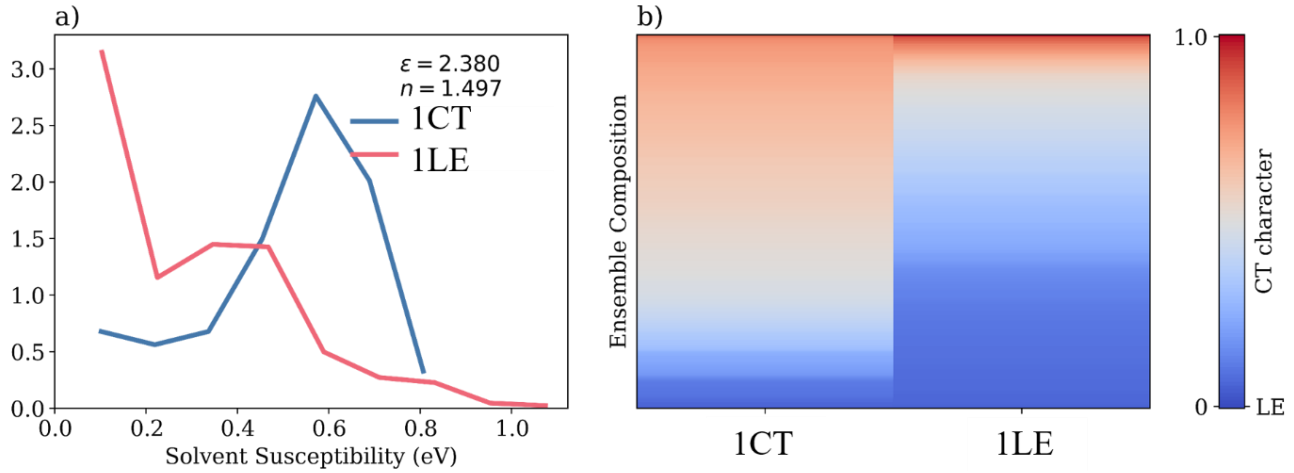

Figure S2. a) Distribution of solvent susceptibilities for CT and LE ensembles. b) Heatmap visualization of susceptibility distributions. Lower susceptibilities are associated with more localized states, whereas higher susceptibilities are associated with stronger CT character. In both cases some degree of CT/LE mixture can be seen, even though a specific kind of transition is predominant in each case.

2.3 Ultraviolet-visible absorption and photoluminescence spectra

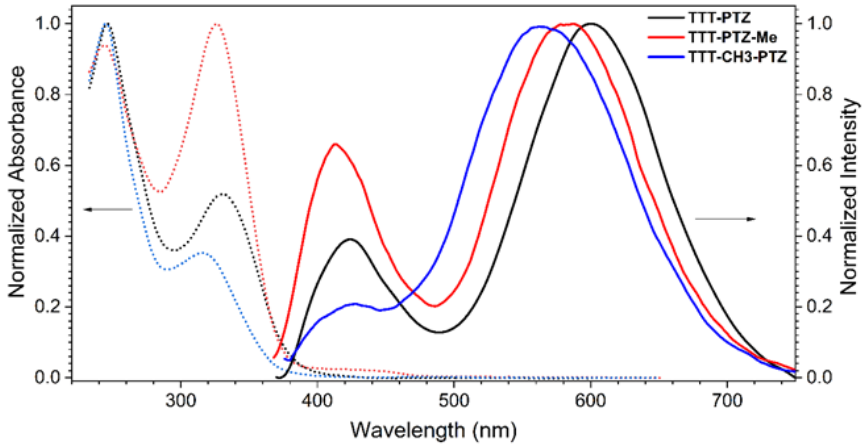

Figure S3. UV-vis (dashed) and fluorescence spectra (solid) of TTT emitters in 1.0×10^{-5} M DCM solution.

2.4 Simulation of fluorescence spectrum of TTT-PTZ

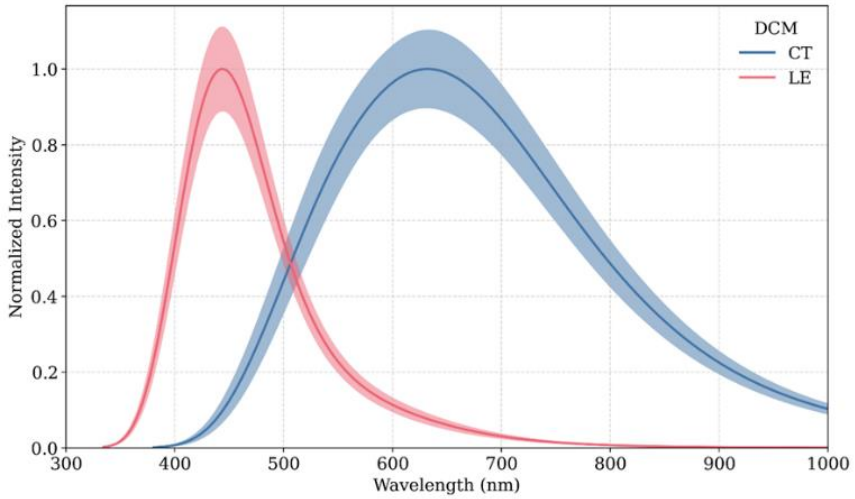

Figure S4. Simulated fluorescence spectrum of ^{1}CT (blue) and ^{1}LE (red) states of **TTT-PTZ** in DCM.

Table S1. Ground-state energies of **TTT-CH$_3$-PTZ** in the gas phase for various conformations.

Conformation	**TTT-CH3-PTZ**
QA-QE-QE	-4274.31387856
QA-QA-QE	-4274.31376072
QA-QA-QA	-4274.31284645
QE-QE-QE	-4274.31270710

3. OLED devices additional data

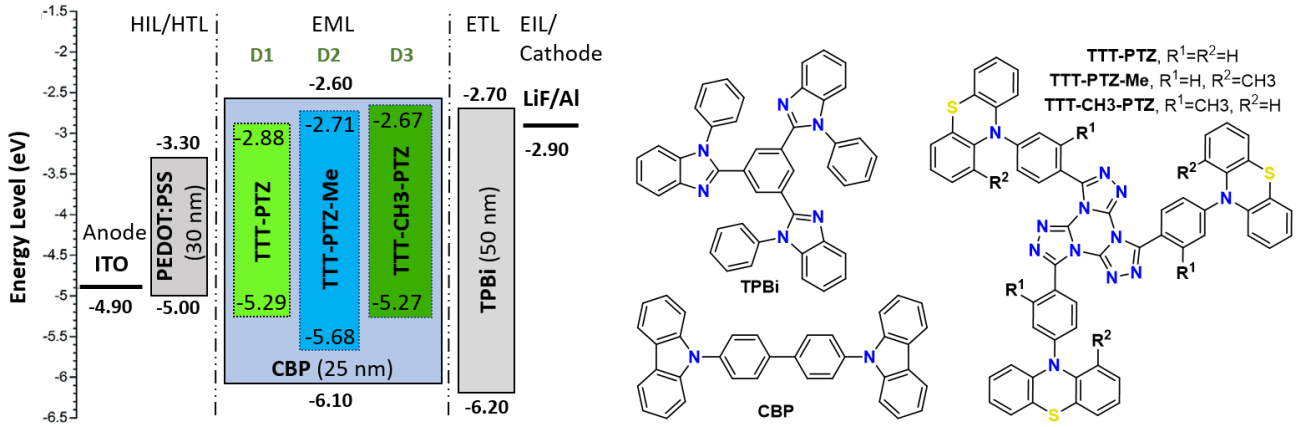

Figure S5. Schematic energy level diagrams of the devices (1-3) investigated in this study and chemical structures of the materials used for device fabrication.

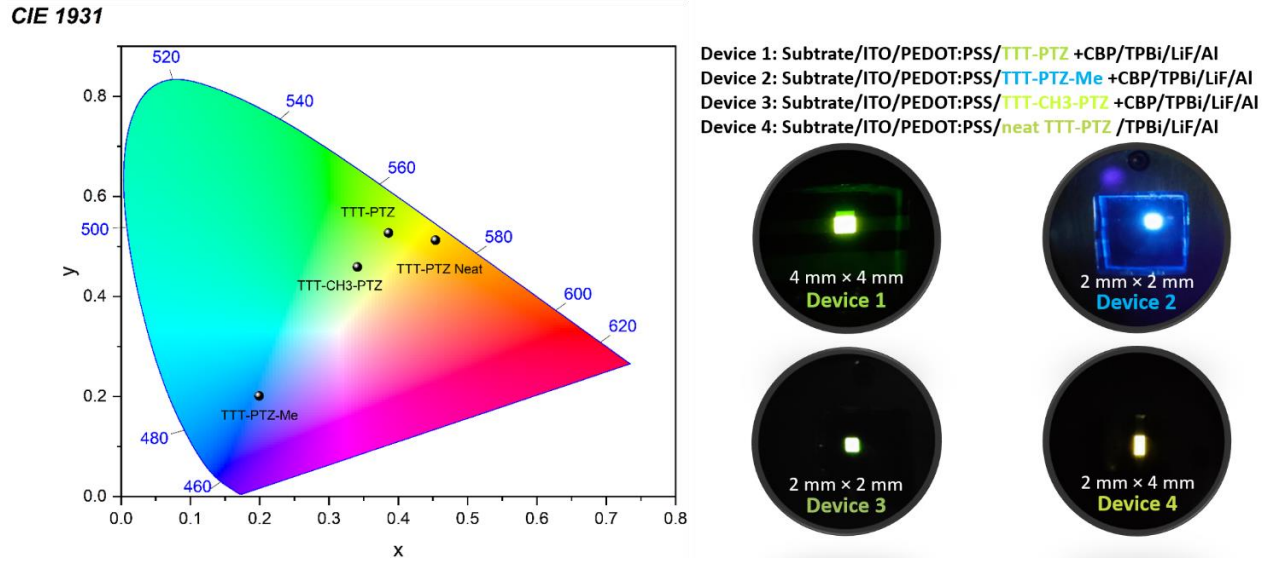

Figure S6. CIE coordinates of fabricated devices (1-4). Device 1: **TTT-PTZ** (0.39, 0.53); Device 2: **TTT-PTZ-Me** (0.20, 0.20); Device 3: **TTT-CH3-PTZ** (0.34, 0.46); Device 4: neat **TTT-PTZ** (0.45, 0.51). Devices 1-3 have a doping concentration of 10 wt% of the emitters in the CBP host.

4. Experimental section

4.1 Synthetic procedures and spectroscopy data

2-methyl-*N*-phenylaniline: The product was prepared according to a modified literature procedure.[1] Bromobenzene

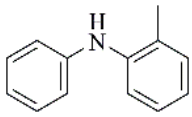

(4.47 g, 157.0 g mol^{-1}, 28.5 mmol, 1 equiv), *o*-toluidine (3.41 g, 107.2 g mol^{-1}, 31.8 mmol, 1.1 equiv), and anhydrous toluene (70 mL) were added via syringe to a degassed mixture of sodium *t*-butoxide (5.48 g, 96.1 g mol^{-1}, 57.0 mmol, 2 equiv) and Pd(dppf)Cl_2.CH_2Cl_2 (698 mg, 816.6 g mol^{-1}, 855 µmol, 3 mol%), then the mixture was bubbled with argon for 15 min. After that, the resulting mixture was stirred at 100 °C, under argon, for 18 hours. The crude product was filtered through a short path of Celite, washed with dichloromethane and the solvent was evaporated. The resulting brown oil was then purified by column chromatography on silica gel in hexanes. Yield: 4.00 g (183.3 g mol^{-1}, 21.8 mmol, 77%) of yellow viscous oil. ^{1}H NMR (300 MHz, $CDCl_3$) δ (ppm): 7.29-7.10 (m, 5H), 7.01-6.87 (m, 4H), 5.39 (br, 1H), 2.26 (s, 3H).

1-methyl-10*H*-phenothiazine: This compound was synthetized following a literature procedure.[1] 1,2-Dichlorobenzene

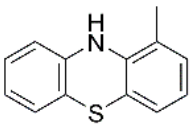

(15 mL) was added via syringe to a degassed mixture of 2-methyl-*N*-phenylaniline (2.10 g, 183.3 g mol^{-1}, 11.5 mmol, 1 equiv), sulfur (840 mg, 32.1 g mol^{-1}, 26.2 mmol, 2.3 equiv), and iodine (100 mg, 253.8 g mol^{-1}, 394 µmol, 3.4 mol%). Then argon was bubbled for 30 min and the resulting mixture was stirred at 180 °C for 18 hours. The crude product was purified by column chromatography on silica gel in hexanes (to remove 1,2-dichlorobenzene) then hexanes-$CHCl_3$, (7:3). Yield: 650 mg (213.3 g mol^{-1}, 3.05 mmol, 27%) of bright yellow solid. ^{1}H NMR (300 MHz, $CDCl_3$) δ (ppm): 7.05-6.96 (m, 2H), 6.88 (d, 2H, *J*= 8Hz) 6.84 (dt, 1H, *J*= 8Hz, 0.9Hz), 6.75 (t, 1H, *J*= 8Hz), 6.61 (dd, 1H, *J*= 8Hz, 1.2Hz), 5.82 (br, 1H), 2.25 (s, 3H).

Procedure for the Buchwald-Hartwig amination: The appropriate aromatic amine (1.2 equiv), the corresponding nitrile (1 equiv), sodium *t*-butoxide (1.2 equiv) and anhydrous toluene were added to a Schlenk tube and degassed. Then, Tris(dibenzylideneacetone)dipalladium(0) (2 mol%) and Tri-*tert*-butylphosphonium tetrafluoroborate (4 mol%) were added under a stream of argon gas at room temperature. The reaction mixture was stirred and heated to 110 °C, under argon, for 24 hours. After that, the insoluble part was removed by filtration and the solvent was concentrated under reduced pressure to get the crude product, which was purified as shown in each product data.

4-(10*H*-phenothiazin-10-yl)benzonitrile (CN-PTZ): CN-PTZ was prepared, according to the amination procedure, from

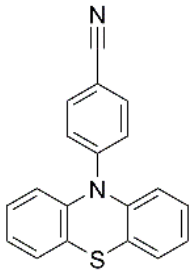

10*H*-phenothiazine (4.88 g, 199.3 g mol^{-1}, 24.5 mmol) and 4-bromobenzonitrile (3.71 g, 182.0 g mol^{-1}, 20.4 mmol) in anhydrous tolune (45 mL) and purified by flash column chromatography on silica gel in hexanes-DCM (8:2). Yield: 2.81 g (300.4 g mol^{-1}, 9.35 mmol, 46%) of white solid. ^{1}H NMR (300 MHz, acetone-d_6) δ (ppm): 7.66 (AA'XX', 2H), 7.52 (m, 2H), 7.39 (m, 4H), 7.29 (m, 2H), 7.18 (AA'XX',

2H); $^{13}C\{^{1}H\}$ NMR (75 MHz, acetone-d_6) δ (ppm): 149.7, 142.1, 134.5, 132.9, 129.5, 128.6, 127.1, 126.5, 119.6, 118.6, 105.5.

4-(1-methyl-10*H*-phenothiazin-10-yl)benzonitrile (CN-PTZ-Me): CN-PTZ-2Me was obtained, following the amination procedure, from 1-methyl-10*H*-phenothiazine (650 mg, 213.3 g mol^{-1}, 3.05 mmol, 1 equiv) and excess of 4-bromobenzonitrile (834 mg, 182.0 g mol^{-1}, 4.58 mmol, 1.5 equiv) in anhydrous tolune (30 mL), then purified by flash column chromatography on silica gel in hexanes-EA (8:2). Yield: 500 mg (314.4 g mol^{-1}, 1.59 mmol, 52%) of white solid. ^{1}H NMR (300 MHz, acetone-d_6) δ (ppm): 7.75 (dd, 1H, *J*= 8 Hz, 1Hz), 7.65 (dd, 1H, *J*= 8Hz, 1Hz), 7.58-7.46 (m, 2H), 7.53 (AA'XX', 2H), 7.44-7.36 (m, 2H), 7.31 (t, 1H, *J*= 8Hz), 6.73 (AA'XX', 2H), 2.39 (s, 3H). $^{13}C\{^{1}H\}$ NMR (75 MHz, $CDCl_3$) δ (ppm): 149.2, 141.0, 139.2, 137.1, 136.9, 136.6, 133.5, 129.5, 129.4, 129.0, 127.5, 127.2, 127.1, 127.0, 119.9, 113.3, 102.2. 18.1.

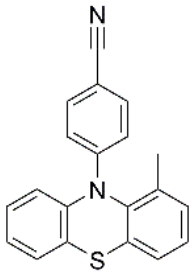

2-methyl-4-(10*H*-phenothiazin-10-yl)benzonitrile (CN-CH_3PTZ): CN-CH_3PTZ was synthesized, according to the amination procedure, from 10*H*-phenothiazine (2.44 g, 199.3 g mol^{-1}, 12.2 mmol) and 4-bromo-2-methylbenzonitrile (2.00 g, 196.0 g mol^{-1}, 10.2 mmol) in anhydrous toluene (25 mL) and isolated pure from flash column chromatography on silica gel in hexanes-DCM (3:1). Yield: 1.76 g (314.4 g mol^{-1}, 5.61 mmol, 55%) of white solid. ^{1}H NMR (300 MHz, acetone-d_6) δ (ppm): 7.63 (d, 1H, *J*= 9Hz), 7.46 (dd, 2H, *J*= 8Hz, 1.5Hz), 7.35 (dd, 1H, *J*= 9Hz, 1.5Hz), 7.33 (dd, 1H, *J*= 8Hz, 1.6Hz), 7.27-7.19 (m, 4H), 7.12 (d, 1H, *J*= 2.5Hz), 7.04 (dd, 1H, *J*= 9Hz, 2.5Hz), 2.43 (s, 3H). $^{13}C\{^{1}H\}$ NMR (75 MHz, acetone-d_6) δ (ppm): 149.1, 144.5, 142.4, 134.9, 131.6, 129.2, 128.5, 126.7, 125.5, 120.9, 118.7, 117.8, 107.0, 20.7.

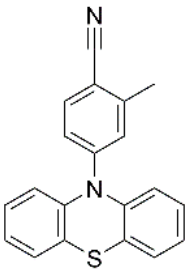

General Procedure for the Synthesis of Tetrazoles

The mixture of corresponding nitrile (1 equiv), ammonium chloride (6 equiv), sodium azide (6 equiv), and DMF was strong stirring at 120 °C, under argon, for 24-36 hours. The reaction progress was monitored by thin layer chromatography (TLC). Then the reaction mixture was poured into a mixture of water/ice and the pH was adjusted around 2, with concentrated aqueous hydrochloric acid. The precipitate was filtered off, washed with plenty of water, and dried. Then the crude product was boiled in dichloromethane (to remove remaining unreacted nitrile).

10-(4-(2*H*-tetrazol-5-yl)phenyl)-10*H*-phenothiazine (TET-PTZ): the tetrazole **TET-PTZ** was synthetized, according to the general procedure, from 4-(10*H*-phenothiazin-10-yl)benzonitrile (2.01 g, 300.4 g mol^{-1}, 6.70 mmol) in DMF (20 mL), and recrystallized from acetone-EA to yield 1.23 g (343.4 g mol^{-1}, 3.58 mmol, 53%) of light yellow crystals. ^{1}H NMR (300 MHz, acetone-d_6) δ (ppm): 8.27 (AA'XX', 2H), 7.52 (AA'XX', 2H), 7.27 (dd, 2H, *J*= 8Hz, 1.7Hz), 7.15 (dt, 2H, *J*= 8Hz, 1.7Hz), 7.06 (dt, 2H, *J*= 8Hz, 1.3Hz), 6.77 (dd, 2H, *J*= 8Hz, 1.3Hz). $^{13}C\{^{1}H\}$ NMR (75 MHz, acetone-d_6) δ (ppm): 146.2, 143.9, 130.1, 128.3, 128.2, 126.9, 126.2, 125.1, 123.0, 121.1.

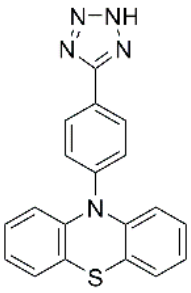

10-(4-(2*H*-tetrazol-5-yl)phenyl)-1-methyl-10*H*-phenothiazine (TET-PTZ-Me): the tetrazole **TET-PTZ-Me** was obtained,

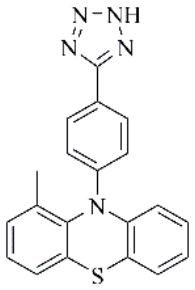

following the general procedure, from 4-(1-methyl-10*H*-phenothiazin-10-yl)benzonitrile (500 mg, 314.4 g mol^{-1}, 1.59 mmol) in DMF (5 mL), yielding 215 mg (357.4 g mol^{-1}, 602 µmol, 38%) of light yellow solid. ^{1}H NMR (300 MHz, acetone-d$_6$) δ (ppm): 7.89 (AA'XX', 2H), 7.78 (dd, 1H, *J*= 8Hz, 1.4Hz), 7.64 (dd, 1H, *J*= 8Hz, 1.4Hz), 7.55 (dt, 1H, *J*= 8Hz, 1.5Hz), 7.51-7.46 (m, 1H), 7.42- 7.39 (m, 1H), 7.40 (dt, 1H, *J*= 8Hz, 1.4Hz), 7.31 (t, 1H, *J*= 8Hz), 6.80 (AA'XX', 2H), 2.43 (s, 3H). ^{13}C{^{1}H} NMR (75 MHz, $CDCl_3$) δ (ppm): 151.2, 148.6, 141.5, 140.5, 139.7, 137.3, 137,0, 136.7, 131.4, 129.4, 129.3, 129.2, 127.3, 126.9, 126.8, 126.79, 114.9, 112.9, 18.3.

10-(3-methyl-4-(2*H*-tetrazol-5-yl)phenyl)-10*H*-phenothiazine (TET-CH$_3$PTZ): the tetrazole **TET-CH$_3$PTZ** was prepared,

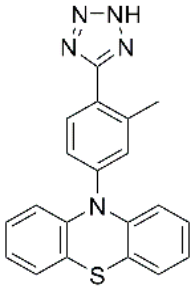

according to the general procedure, from 2-methyl-4-(10*H*-phenothiazin-10-yl)benzonitrile (1.41 g, 4.50 mmol) in DMF (13 mL). Yield: 836 mg (357.4 g mol^{-1}, 2.34 mmol, 52%) of white solid. ^{1}H NMR (300 MHz, acetone-d$_6$) δ (ppm): 8.01 (d, 1H, *J*= 9Hz), 7.41 (d, 1H, 2Hz), 7.36 (dd, 1H, *J*= 9Hz, 2Hz), 7.21 (dd, 2H, *J*= 8Hz, 1.6Hz), 7.10 (dt, 2H, *J*= 8Hz, 1.6Hz), 7.05-6.97 (m, 2H), 6.65 (d, 2H, *J*= 8Hz), 2.65 (s, 3H).

5. Copies of NMR Charts of final compounds

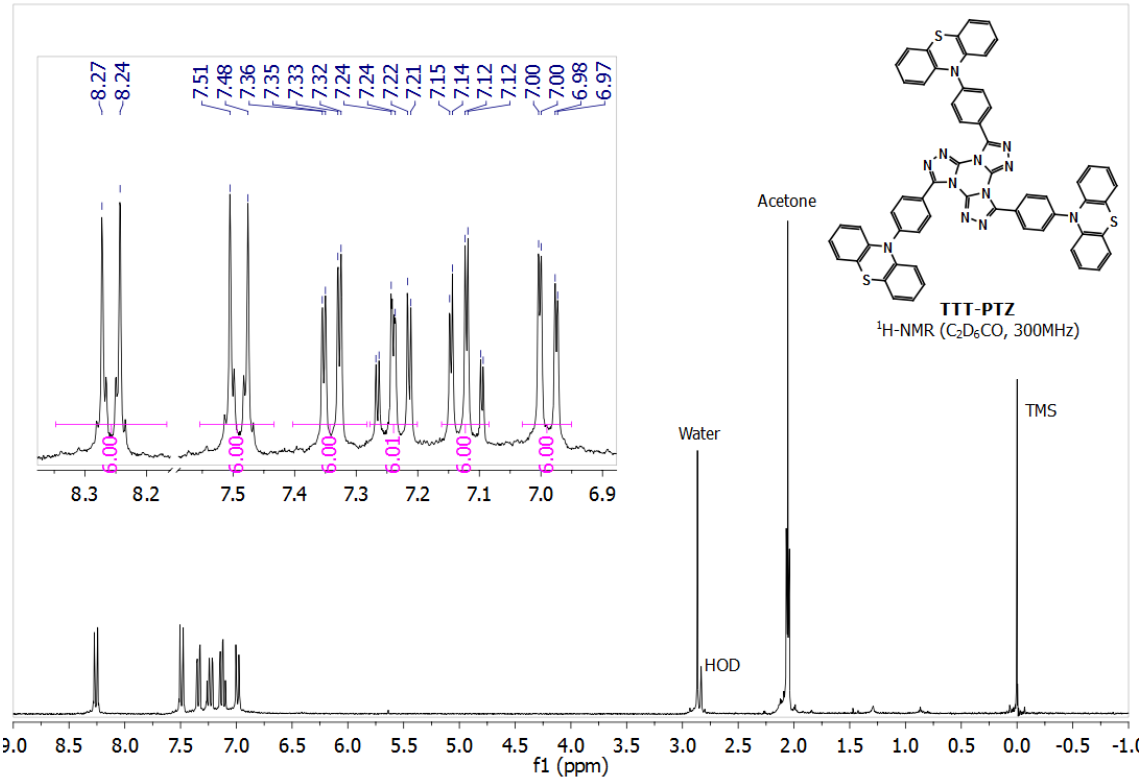

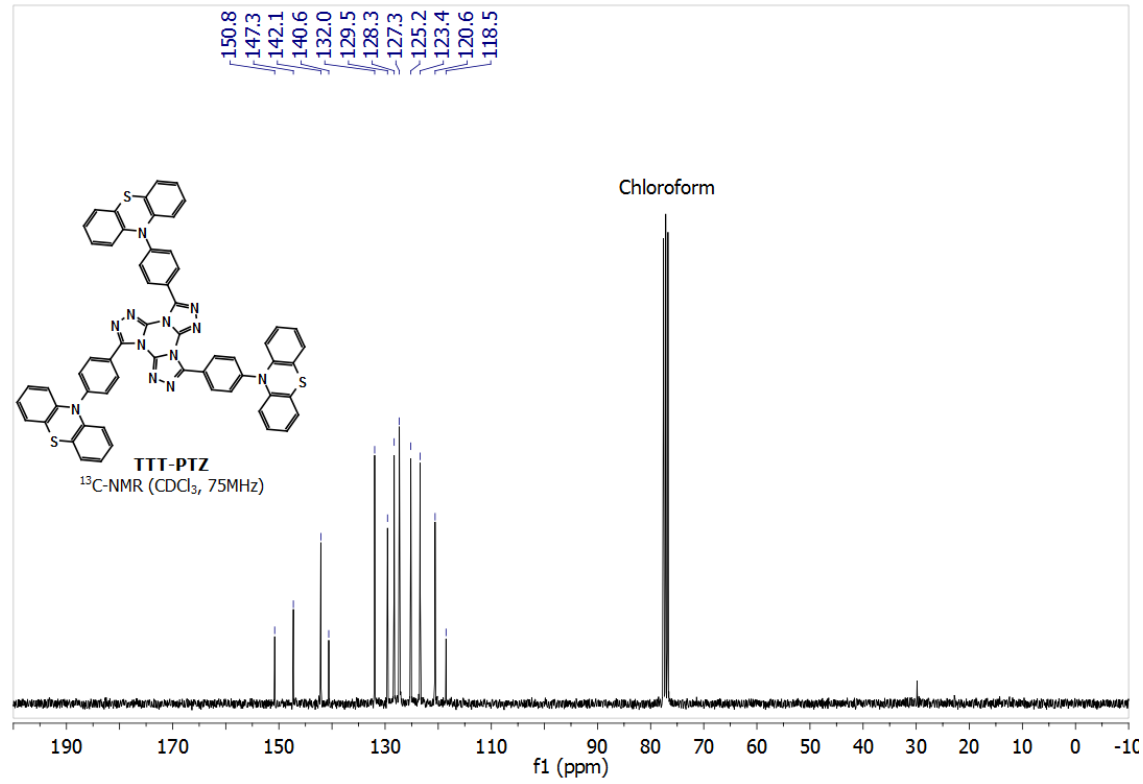

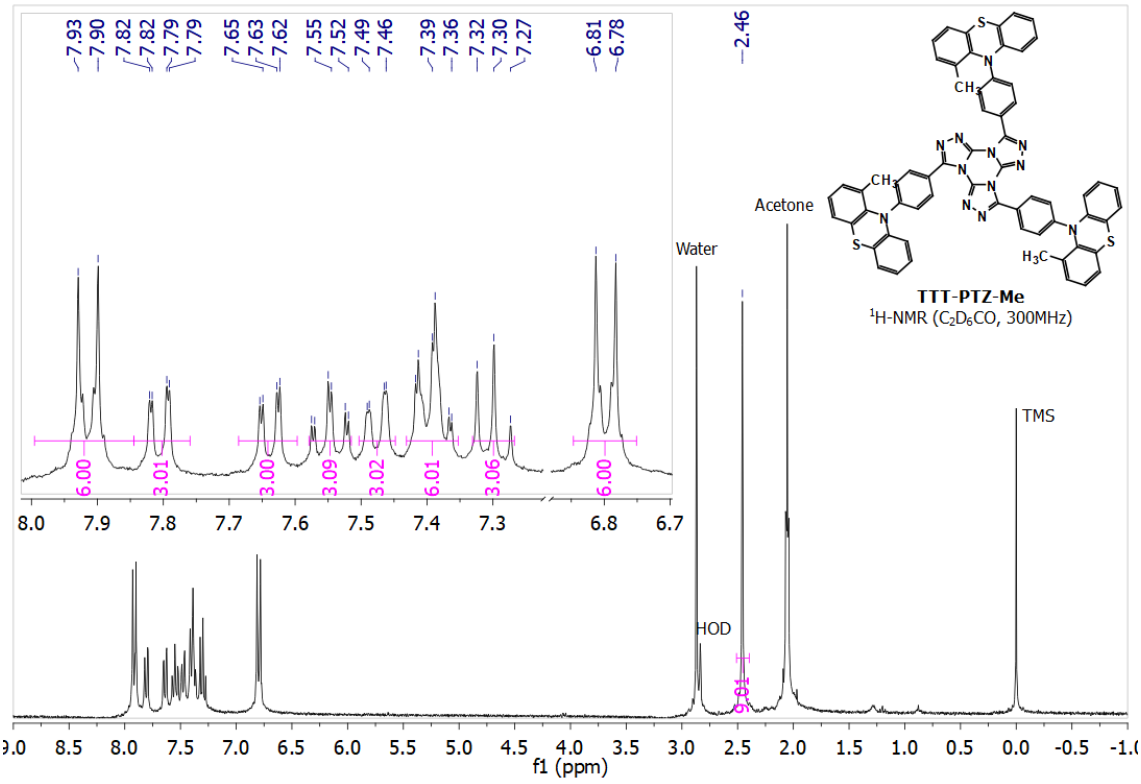
7.93
7.90
7.82
7.82
7.79
7.79
7.65
7.63
7.62
7.55
7.52
7.49
7.46
7.39
7.36
7.32
7.30
7.27
6.81
6.78
2.46
Water
Acetone
TMS
HOD
6.00
3.01
3.00
3.09
3.02
6.01
3.06
6.00
9.01
f1 (ppm)
TTT-PTZ-Me
1H-NMR (C2D6CO, 300MHz)

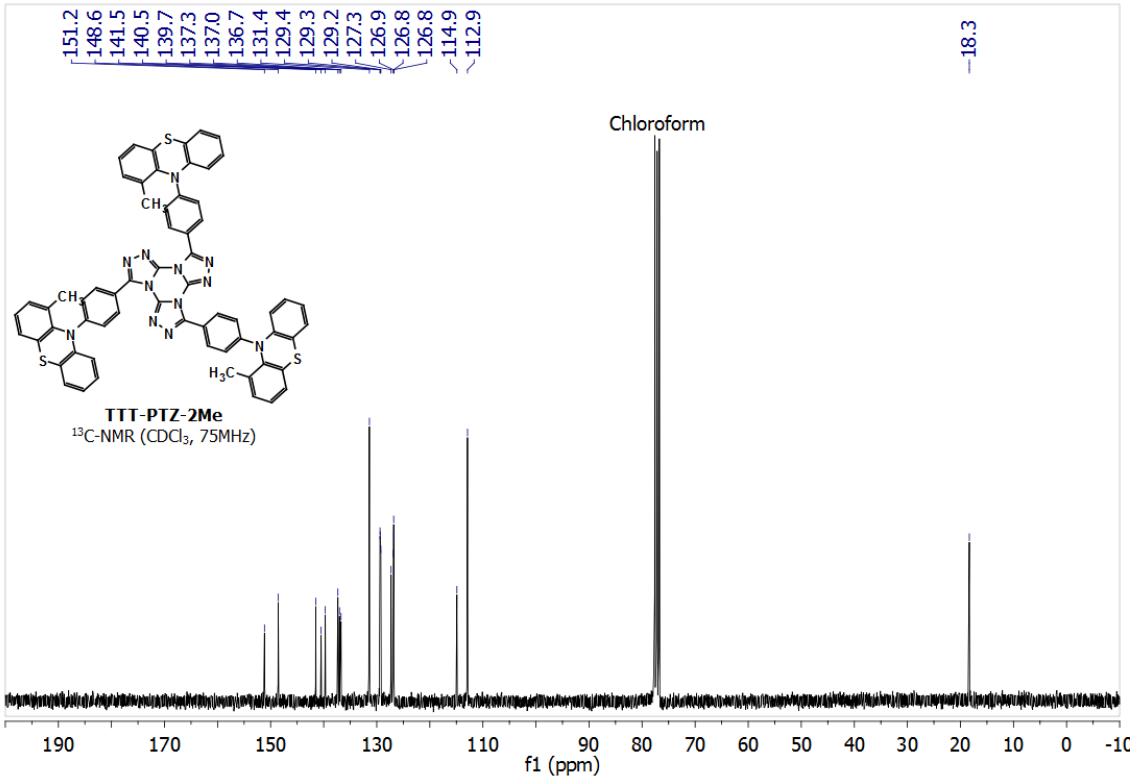
151.2
148.6
141.5
140.5
139.7
137.3
137.0
136.7
131.4
129.4
129.3
129.2
127.3
126.9
126.8
126.8
114.9
112.9
18.3
Chloroform
f1 (ppm)
TTT-PTZ-2Me
13C-NMR (CDCl3, 75MHz)

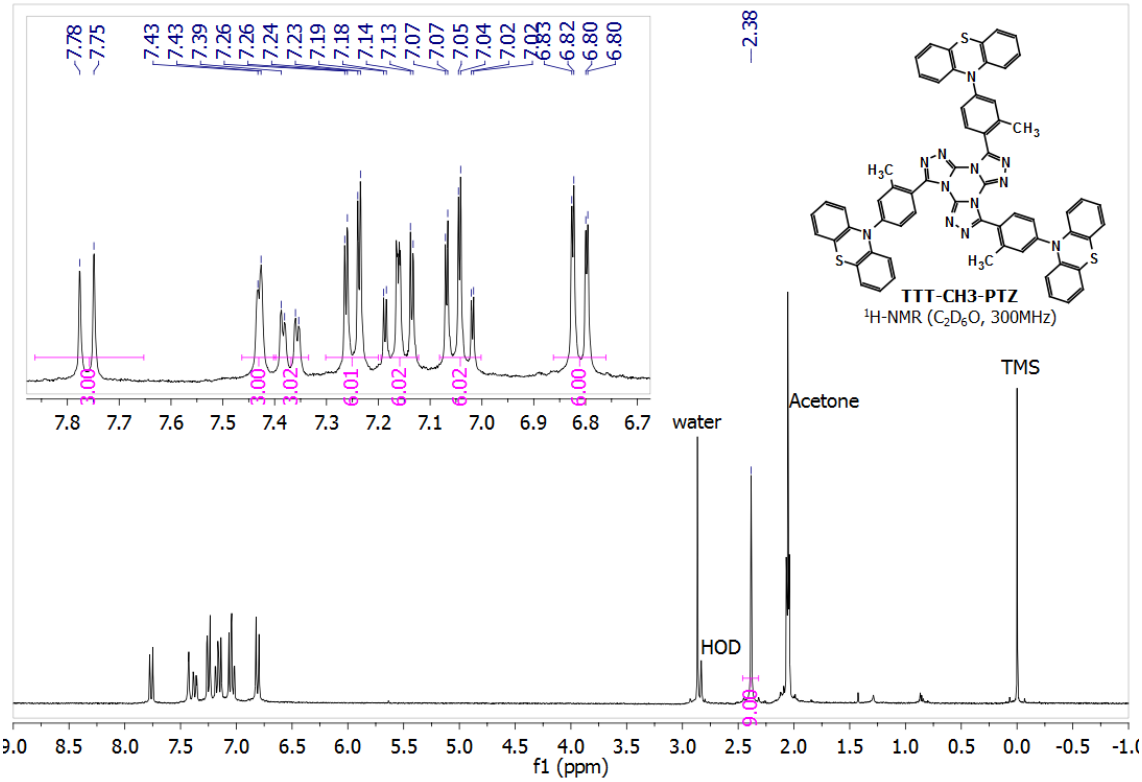
7.78
7.75
7.43
7.43
7.39
7.26
7.26
7.24
7.23
7.19
7.18
7.14
7.13
7.07
7.07
7.05
7.04
7.02
7.02
6.83
6.82
6.80
6.80
2.38
3.00
3.00
3.02
6.01
6.02
6.02
6.00
water
Acetone
TMS
HOD
9.08
TTT-CH3-PTZ
1H-NMR (C2D6O, 300MHz)
f1 (ppm)

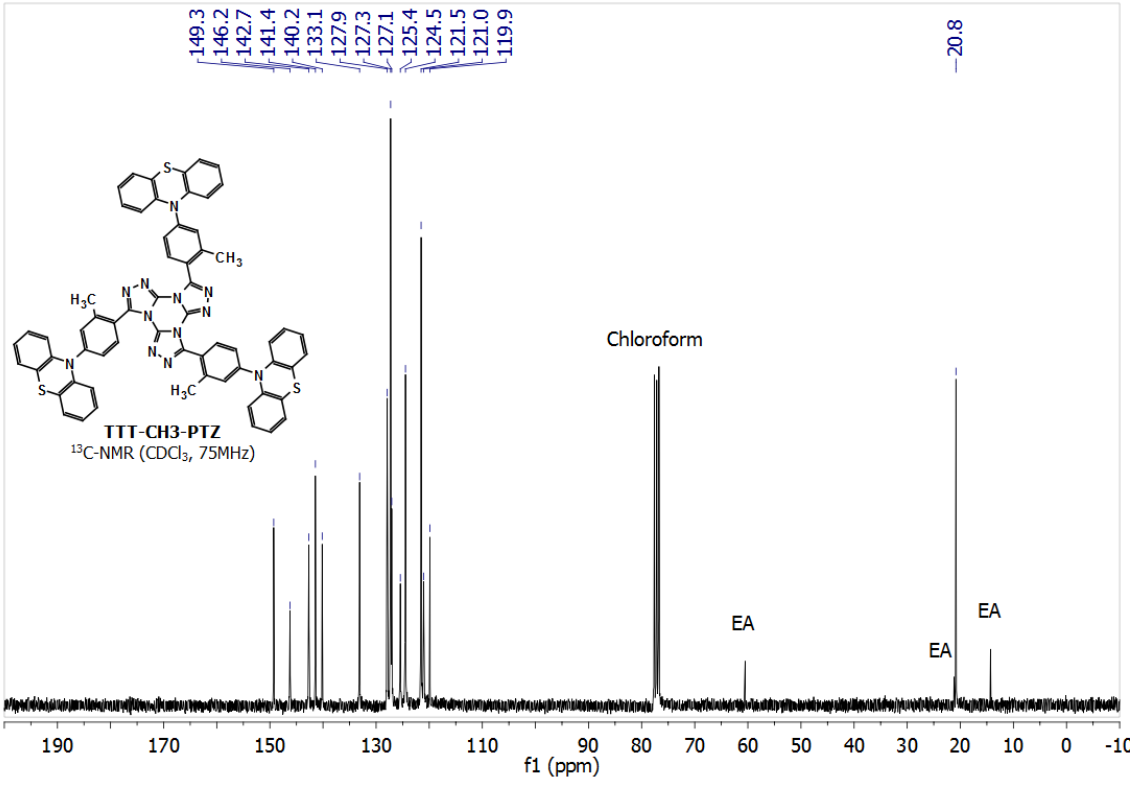
149.3
146.2
142.7
141.4
140.2
133.1
127.9
127.3
127.1
125.4
124.5
121.5
121.0
119.9
20.8
Chloroform
EA
EA
EA
TTT-CH3-PTZ
13C-NMR (CDCl3, 75MHz)
f1 (ppm)

6. Computational details

Conformation search

The present study employed a stochastic algorithm to systematically investigate potential energy surfaces and identify diverse molecular conformations associated with energy minima. The algorithm starts with a random sampling of N_c molecular geometries from the distribution of harmonic oscillators at temperature T. This distribution is given by:[4]

$$\rho(\vec{R},T) = \prod_{i=1}^{3N-6}\left(\frac{\mu_i\omega_i}{2\pi\hbar\sinh\left(\frac{\hbar\omega_i}{k_bT}\right)}\right)exp\left(-\frac{\mu_i\omega_i}{\hbar}R_i^2\tanh\frac{\hbar\omega_i}{2k_bT}\right)$$

Where, N represents the number of atoms in the molecule, μ_i and ω_i are the reduced mass and the angular frequency of the i[th] normal mode, respectively. k_b is the Boltzmann constant, and R_i, is the normal coordinate. These parameters are derived from a normal mode calculation, are used as input for the algorithm. The initial sampling temperature, T_0, is automatically determined to ensure that the thermal energy (k_bT) of the molecule matches the energy of the fortieth normal mode ($\hbar\omega_{40}$) of the conformer, or the last mode if 3N−6 < 40. The selection of the fortieth mode is arbitrary and was determined through trial and error during the search process.

After optimizing each sampled geometry, the resulting structure's adjacency matrix is compared to that of the input molecule. If this process produces a distinct molecule, the structure is discarded; otherwise, the algorithm extracts the three rotational constants (B_i) of the resulting conformer. As these rotational constants are directly associated with the moments of inertia (I_i) of the molecule $B_i = \frac{\hbar}{4\pi cI_i}$), they serve as key parameters for categorizing candidate molecules into distinct groups.

The initial classification involves comparing the rotational constants of each molecule with those of the initial conformation. An initial criterion is set at 1/1000 of the rotational constants from the original input. If any of the three constants for the two molecules differ by more than this criterion, the molecule in question is considered to correspond to a different conformation. Conversely, if the differences are within the established criterion, the molecule is assigned to one of the previously identified categories. Following this assignment, the algorithm calculates the averages and standard deviations of the rotational constants for all molecules identified so far within the same classification. These averages then serve as representative values for that particular conformation. Simultaneously, the classification criteria are updated to the minimum non-zero value between the original criterion and twice the calculated standard deviation for each rotational constant.

After the classification of all the molecules, and if no new conformer is identified, the algorithm increases its temperature by ΔT and samples N_c new structures, and the process describe above is performed again. Conversely, if a new conformation is detected, a normal mode analysis is conducted on the new conformer, serving as the starting point for subsequent geometry sampling. This iterative cycle is performed for N_r rounds, after which the algorithm presents the identified conformers, their average energies, and Boltzmann populations at 300 K.

In this study, the conformational search algorithm was executed for each analyzed molecule over $N_r = 10$ rounds, with $N_c = 10$ geometries sampled in each round and a temperature increment of $\Delta T = \frac{T_0}{10K}$. For the conformation search, the semi-empirical method PM6 was used. The 10 selected configurations were then re-optimized using the functional LC-ω hPBE coupled to the basis 6-31G(d,p) and the long-range parameter is set to 0.1749 $bohr^{-1}$.

7. References

[1] J. S. Ward, R. S. Nobuyasu, A. S. Batsanov, P. Data, A. P. Monkman, F. B. Dias, M. R. Bryce, *Chemical Communications* **2016**, *52*, 2612-2615.

[2] T. Wu, T. Kim, B. Yin, K. Wang, L. Xu, M. Zhou, D. Kim, J. Song, *Chemical Communications* **2019**, *55*, 11454-11457.

[3] S. B. Mane, C.-F. Cheng, A. A. Sutanto, A. Datta, A. Dutta, C.-H. Hung, *Tetrahedron* **2015**, *71*, 7977-7984.

[4] R. P. Feynman, Statistical Mechanics: a Set of Lectures (Advanced Book Classics) Westview Press **1998**.